

Cluster-Based MIMO Channel Model Parameters Extracted from Indoor Time-Variant Measurements

Nicolai Czink^{1,2}, Ernst Bonek^{1,2}, Lassi Hentilä³, Jukka-Pekka Nuutinen³, Juha Ylitalo^{3,4}

¹Institut für Nachrichtentechnik und Hochfrequenztechnik, Technische Universität Wien, Vienna, Austria

²Forschungszentrum Telekommunikation Wien (ftw.), Vienna, Austria

³Elektrobit Testing Ltd., Oulu, Finland

⁴Centre for Wireless Communications, Oulu University, Oulu, Finland

Abstract—This paper presents a complete solution to the problem of how to parametrise cluster-based stochastic MIMO channel models from measurement data, with minimum user intervention.

The method comprises the following steps: (i) identify clusters in measurement data, (ii) identify the optimum number of clusters, (iii) track clusters over consecutive time snapshots, (iv) estimate cluster parameters. These parameters are given as estimated probability density functions of the cluster power, cluster positions, delay and angular spreads of clusters and the number of paths within a cluster.

Applied to high-resolution indoor MIMO measurement data at 5.2 GHz and at 2.55 GHz, the method yields coherent results of the obtained cluster parameters.

I. INTRODUCTION

In order to find schemes that exploit the opportunities offered by the wireless MIMO channel, MIMO channel models that are detailed yet tractable are strongly needed. A promising approach involves cluster-based MIMO channel models [1].

Multi-path clusters were defined as “propagation paths that show similar angles and delay”, and were observed in measurements, e.g. by [2], [3]. It was shown in [4] that channel models disregarding clusters overestimate the channel capacity.

Recent MIMO channel models took the idea of clusters several steps further [5]. The issue that was left open is the problem of identifying and parametrising clusters from measurements. Previous work used visual inspection to identify clusters [3], but this method lacks an accurate definition of a cluster. Moreover, it is inefficient when using a large amount of measurement data; for multi-dimensional data the visual approach becomes impossible.

First attempts to automatically identify clusters were introduced in [6], where a heuristic clustering algorithm was used, based on standard clustering methods [7]. This algorithm was further improved in [8], [9]. Still the issue of tracking clusters over multiple time snapshots was left open.

To our knowledge this is the first paper to present a full framework for identification and characterisation of cluster parameters from measurement data, including experimental results. We proceed stepwise: (i) the clustering is based on a parametric cluster model, which is introduced in Section II; (ii) parametric measurement data is clustered using a specific clustering algorithm (Section III-A); (iii) the optimum number

of clusters is evaluated (Section III-B); (iv) clusters are tracked and their parameters are estimated (Section III-C).

We apply our framework to indoor measurement data in Section IV and present the obtained cluster parameters in Section V.

II. PARAMETRIC CLUSTER CHANNEL MODEL

In this paper we consider the discrete paths of the propagation channel, which can be resolved by high-resolution parameter estimation techniques. Paths that can not be resolved may be treated according to [10] as “dense multi-path”.

A. Path model

One discrete path is described by its parameters, the complex-valued path weight, γ , delay, τ , and azimuth and elevation angles of arrival and departure, AoA φ_{Rx} , EoA ϑ_{Rx} , AoD φ_{Tx} , EoD ϑ_{Tx} , respectively, collected in a path parameter vector

$$\boldsymbol{\theta} = [\gamma \ \tau \ \varphi_{\text{Rx}} \ \vartheta_{\text{Rx}} \ \varphi_{\text{Tx}} \ \vartheta_{\text{Tx}}].$$

We describe one snapshot of the environment by all paths contributing to it

$$\Theta = \underset{l=0}{\overset{L}{\Xi}} \boldsymbol{\theta}_l,$$

where L is the number of paths in the considered snapshot, $\boldsymbol{\theta}_l$ contains the parameters of the l th path and $\Xi_{l=1}^L$ is stacking the rows of the path parameter vectors, i.e. $\Xi_{l=0}^L \boldsymbol{\theta}_l \triangleq [\boldsymbol{\theta}_1^T \dots \boldsymbol{\theta}_L^T]^T$.

B. High-resolution parameter estimators

High resolution parameter estimators also use this model to estimate the (resolvable) paths in a given snapshot. Their output is the estimated multi-path structure of the channel $\tilde{\Theta}$. We will use these estimates as input for our model.

C. Cluster-based path model

We now propose to model the scenario by using *multi-path clusters*, consisting of propagation paths showing the *same parameter statistics*. Note that, in this concept, clusters are treated as a *means to model the channel*.

We model one snapshot of a scenario as

$$\tilde{\Theta} = \underset{k=1}{\overset{K}{\Xi}} \tilde{\Theta}_k, \quad (1)$$

with $\tilde{\Theta}_k$ denoting the *modelled* cluster parameter matrices, and K denoting the number of clusters in the environment.

The modelled cluster parameter matrices $\tilde{\Theta}_k$ collect the parameters of the propagation paths of the k th cluster,

$$\tilde{\Theta}_k = \sum_{l=1}^{L_k} \tilde{\theta}_{kl}^T,$$

with L_k paths within the k th cluster.

The parameters of all paths within one cluster are modelled statistically by following distributions¹:

$$\begin{aligned} \tilde{\tau}_{kl} &\sim \mathcal{N}(\tilde{\mu}_{\tau_k}, \tilde{\sigma}_{\tau_k}^2) \\ \tilde{\varphi}_{\text{Rx},kl} &\sim \mathcal{N}(\tilde{\mu}_{\varphi_{\text{Rx},k}}, \tilde{\sigma}_{\varphi_{\text{Rx},k}}^2) \\ \tilde{\vartheta}_{\text{Rx},kl} &\sim \mathcal{N}(\tilde{\mu}_{\vartheta_{\text{Rx},k}}, \tilde{\sigma}_{\vartheta_{\text{Rx},k}}^2) \\ \tilde{\varphi}_{\text{Tx},kl} &\sim \mathcal{N}(\tilde{\mu}_{\varphi_{\text{Tx},k}}, \tilde{\sigma}_{\varphi_{\text{Tx},k}}^2) \\ \tilde{\vartheta}_{\text{Tx},kl} &\sim \mathcal{N}(\tilde{\mu}_{\vartheta_{\text{Tx},k}}, \tilde{\sigma}_{\vartheta_{\text{Tx},k}}^2) \\ \text{abs}(\tilde{\gamma}_{kl}) &= \sqrt{\frac{\tilde{\rho}_k}{\tilde{L}_k}} \\ \arg(\tilde{\gamma}_{kl}) &\sim \mathcal{U}([- \pi \dots \pi]) \end{aligned}$$

Hence, the *cluster parameters* \mathcal{C}_k consist only of the mean values and variances of the different parameters, which we collect in $\tilde{\mu}_k$ and $\tilde{\sigma}_k$, respectively, the power of the cluster, $\tilde{\rho}_k$, and the number of paths, \tilde{L}_k , within the k th cluster, i.e. $\mathcal{C}_k = \{\tilde{\mu}_k, \tilde{\sigma}_k, \tilde{\rho}_k, \tilde{L}_k\}$, with $k = 1 \dots K$. Note that, if the number of clusters approaches the total number of paths in the snapshot, this model always matches.

Our task is to find an estimator for best fitting the number of clusters K and the respective cluster parameters \mathcal{C}_k to the path parameters obtained from measurements $\hat{\Theta}$.

III. CLUSTER PARAMETER ESTIMATOR

Reflecting the given multi-path structure of a channel with the cluster-based model is not easy. Using too few clusters will not reflect the environment correctly. On the other hand, one needs to track clusters over several snapshots in time to get a basic estimate of their parameters. When using too many clusters, tracking is not possible. Hence, we have to solve two problems: (i) find the correct number of clusters, (ii) find the optimum agglomeration of paths into clusters, in order to minimise the model mismatch.

We solve both problems with the following procedure. First, we specify a minimum and maximum number of clusters, where we typically choose $K_{\min} = 2$ and $K_{\max} = 20$. Subsequently, we cluster each single snapshot for all $K = [K_{\min} \dots K_{\max}]$. Then we find the smallest possible number of clusters K_{opt} that describes the scenario with sufficient accuracy.

A. Clustering algorithm

As clustering algorithm we chose the KPowerMeans algorithm introduced in [9]. This algorithm is quite powerful: (i) it provides *joint* multi-dimensional clustering of propagation

path parameters (even if the parameters come in different units like delays and angles), (ii) it includes path powers in the clustering process, such that strong paths attract cluster centres more than weak paths². This algorithm also introduces an inherent definition of a cluster:

For a given number of clusters, clusters are chosen such that they minimise the total distance from their centroids.

This implies that, for a given K , clusters are selected such that *the cluster angular and cluster delay spreads are minimised*, which again is consistent with the proposed model in Section II.

The final output of KPowerMeans is the optimum agglomeration of paths to K clusters, where we collected the respective paths to each cluster in the result sets for each snapshot, $\hat{\Theta}_k$.

B. Number of clusters

As we go for modelling the scenario with as few clusters as possible, we define the optimum number of clusters as follows:

The optimum number of clusters is defined by the lowest number of clusters for which it is possible to reflect the given scenario with a certain error threshold.

The algorithm to meet this definition is as follows: For every number of clusters K we extract the cluster parameters \mathcal{C}_k , $k = 1 \dots K$, for this single snapshot (see Section III-C). Subsequently, we generate a number of M modelled snapshots $\hat{\Theta}_m$, $m = 1 \dots M$ according to the obtained parameters. Finally, we calculate the mean mismatch between the modelled scenarios and the true paths³. As a measure how well paths match we use the *environment characterisation metric* (ECM). Each path l is transformed into a normalised parameter domain and is represented by

$$\boldsymbol{\pi}_l = [\tau_l^{(n)} \ x_{\text{Tx},l} \ y_{\text{Tx},l} \ z_{\text{Tx},l} \ x_{\text{Rx},l} \ y_{\text{Rx},l} \ z_{\text{Rx},l}]^T, \text{ and } |\gamma_l|^2,$$

where $x_{(\cdot)}$ describes the x-component of the Tx or Rx angle on the unit sphere, and similar for $y_{(\cdot)}$ and $z_{(\cdot)}$. The delay is normalised such that $\tau_l^{(n)} = \frac{\tau_l}{\max_l \tau_l}$.

We then calculate the mean parameter vector of the snapshot

$$\bar{\boldsymbol{\pi}} = \frac{\sum_{l=1}^L |\gamma_l|^2 \boldsymbol{\pi}_l}{\sum_{l=1}^L |\gamma_l|^2}.$$

The ECM is defined as the covariance of the path parameters

$$\mathbf{C}_{\boldsymbol{\pi}} = \frac{\sum_{l=1}^L |\gamma_l|^2 (\boldsymbol{\pi}_l - \bar{\boldsymbol{\pi}})(\boldsymbol{\pi}_l - \bar{\boldsymbol{\pi}})^T}{\sum_{l=1}^L |\gamma_l|^2}.$$

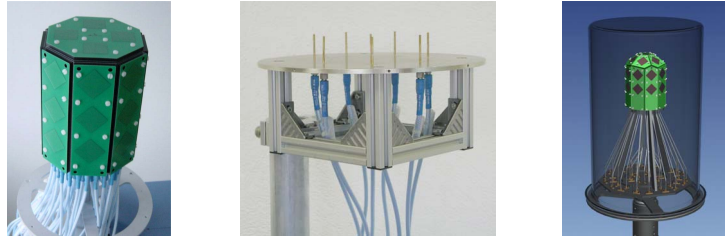
The singular values (SV) σ_d^2 of this metric⁴ can be seen as “fingerprint” of the scenario. The mismatch between the true

²We model each path in one cluster with same power but random phase as is common. In contrast *parameter estimators* typically estimate strong paths at cluster centres and weaker paths around them.

³We call the paths estimated from the measurements as “true” paths in contrast to the “modelled” paths.

⁴with d denoting the SV index

¹ \mathcal{N} , and \mathcal{U} denote the Gaussian and uniform distribution, respectively



(a) 3x8 ODA, 2.55 GHz (b) 7+1 UCA, 2.55 GHz (c) 2x9 ODA, 5.25 GHz

Fig. 1. Antenna arrays. (a) 2.55 GHz omni-directional patch array, (b) 2.55 GHz circular monopole array, (c) 5.25 GHz omni-directional patch array.

and the modelled scenarios is defined as

$$\mathcal{E} = \frac{1}{D} \sum_{d=1}^D |\hat{\sigma}_{d,[dB]}^2 - \tilde{\sigma}_{d,[dB]}^2|,$$

with $\hat{\sigma}_{d,[dB]}^2$ denoting the SVs of the ECM obtained from the true environment, and $\tilde{\sigma}_{d,[dB]}^2$ denoting the SVs of the ECM obtained from the modelled environment.

As we generate M snapshots with the model, we take the mean of the mismatch as the final measure how well the model fits. Finally, the number of clusters is given by the lowest number of clusters where the mean mismatch is beyond a certain error threshold. We empirically set this threshold to 0.3 dB, as evaluations showed that the parameter estimator itself is only able to characterise simulated environments with a minimum error of around 1 dB.

C. Cluster parameters

Using the clustered propagation paths in $\hat{\Theta}_k$, we can estimate the statistical parameters for this cluster by building the sample mean and sample variance for each snapshot. For the delay domain this yields

$$\tilde{\mu}_{\tau_k} = \frac{\sum_{l=1}^{L_k} |\gamma_{kl}|^2 \tau_{kl}}{\sum_{l=1}^{L_k} |\gamma_{kl}|^2}, \text{ and}$$

$$\tilde{\sigma}_{\tau_k} = \sqrt{\frac{\sum_{l=1}^{L_k} |\gamma_{kl}|^2 (\tau_{kl} - \tilde{\mu}_{\tau_k})^2}{\sum_{l=1}^{L_k} |\gamma_{kl}|^2}},$$

and reads similar for all the other dimensions. As number of paths within a cluster we use the number of estimated paths within the cluster, hence $\tilde{L}_k = \hat{L}_k$.

We observed that most clusters exist for more than one snapshot in time, which suggests that the observed clusters are associated to some physical scattering areas. Hence, to capture the time-variance of the cluster parameters, we use a simple tracking algorithm [11] to estimate the cluster parameters over a longer time period. In this paper we average the parameters over the snapshots in which the clusters exist and present the mean cluster parameters of this approach.

IV. MEASUREMENTS

A. Equipment and set-up

In this study we use a wideband radio channel sounder, Prosound CSTM, which utilises periodic pseudo-random binary signals. The sounder is described in more detail in [12].

TABLE I
SOUNDER PARAMETERS

Parameter	2.55 GHz	5.25 GHz
Transmit power [dBm]	26	26
Bandwidth [MHz]	200	200
Chip frequency [MHz]	100	100
Code length [μ s]	2.55	2.55
Channel sampling rate [Hz]	92.6	59.4
Cycle duration [μ s]	1542.24	8415.00

The spread spectrum signal has 100 Mchip/s chip rate and switches through all the antennas with the cycle rates presented in Table I. Thus, sequential radio channel measurement between all possible TX and RX antenna pairs is achieved by antenna switching at both the transmitter and the receiver. The number of antenna elements used is proportional to the cycle rate. The sounder was operated in burst-mode, i.e. after four measuring cycles there was a break to allow real-time data transfer to the control laptop computer. Subsequently, we estimated the propagation paths for every snapshot in time using the ISISTM (Initialisation and Search Improved SAGE) software. This estimation algorithm is based on a super-resolution SAGE algorithm employing maximum likelihood techniques for parameter estimation [13].

The selected antenna arrays illustrated in Figure 1 are able to capture largely the spatial characteristics of the radio channel at *both* link-ends. The 2.55 GHz array (Figure 1a) used at the TX consists of 28 dual-polarised patch elements. The elements are positioned in a way that allows channel probing in the *full* azimuth domain and almost full coverage of the elevation. Only a small cone in space angle along the supporting pole of the array cannot be covered. Figure 1b shows the uniform circular array with 7+1 monopoles used at the RX end at 2.55 GHz. It supports full azimuth direction probing but not the elevation. At 5.25 GHz both TX and RX had 25 element patch arrays shown in Figure 1c, where we used only a subset of 16 antennas at the RX. The properties of these two arrays are similar to the 2.55 GHz patch array. All antennas had been calibrated in an anechoic chamber. The signal model on which ISIS is based is using the array pattern data over rotation of the array as a base to calculate the response of each element to waves impinging from different angles.

B. Scenario

We took numerous measurements and decided to present results from one exemplary route in this paper. It is a medium-sized student laboratory (Figure 2). To facilitate comparison

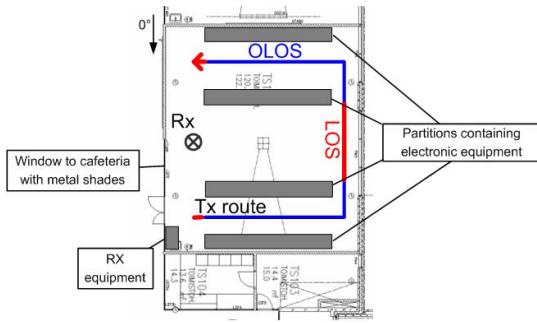


Fig. 2. Measurement route in the medium-sized laboratory; Antenna orientation for 0° is the same for both Rx and Tx.

of results, the same routes were measured on successive measurements with different channel sounder radio modules for the two above mentioned carrier frequencies.

The measurement route changed from LOS (line of sight) to OLOS (direct line of sight obstructed by partitions, equipped with laboratory instruments), back to LOS, then OLOS again and finished with LOS (marked with blue and red colour in Figure 2). The movement speed was around 0.5 m/s. We averaged over 4 cycles, which corresponds to 0.18λ travel for 2.55 GHz and 0.58λ for 5.25 GHz. The operation in burst mode resulted in a separation between two consecutive averaged channel estimates of 0.74λ at 2.55 GHz and 2.4λ at 5.25 GHz.

V. RESULTS

We applied the clustering and tracking algorithm to our data. Then we disregard clusters that could not be tracked (i.e. only exist in one time snapshot).

We estimated the cluster parameters for each time snapshot and calculated the mean values. Then we estimate the probability density functions (pdf) of these parameters⁵. These pdfs can easily be used for stochastic modelling of propagation scenarios. We compare the pdfs in Figure 3 for the LOS and OLOS situations for 2.55 GHz centre frequency (red and blue curves).

Figure 3a shows the pdf of the absolute cluster powers, ρ_k . We observe that the cluster power in the OLOS case is Log-Normal distributed, while it seems to be well approximated by a double-exponential distribution for the LOS situations. Figure 3b shows the distribution of cluster power, ρ_k , relative to the total power of all clusters within one snapshot (corresponding to 0 dB). We observe fewer strong clusters than weak clusters. This is more pronounced in the LOS case. The OLOS case seems to be well-approximated by a Log-Normal behaviour.

Figure 3c shows the average number of paths, L_k , within one cluster. Interestingly, it seems to be independent of LOS or OLOS situations, a number of 5–10 paths being most probable.

The mean cluster AoA $\mu_{\phi_{\text{Rx},k}}$ in Figure 3d serves as a check of plausibility. For LOS, we observe many clusters at 0° and 90° , which corresponds to the start and the middle part of the

⁵Note that we use the abbreviation pdf for *estimated* probability density functions.

route. In addition, for the OLOS case predominant directions are expected due to the specific propagation environment.

Figures 3e,f show the cluster angular spreads for the AoA and AoD, $\sigma_{\phi_{\text{Rx},k}}$, $\sigma_{\phi_{\text{Tx},k}}$, respectively. One can observe two important properties: First, the AoA and AoD spreads seem to have similar statistics. This comes from the fact that Rx and Tx were in the same room. Second, the cluster angular spreads are usually smaller in LOS situations. Figure 5 shows the joint pdf of two evidently correlated parameters: the number of clusters and the cluster AoD rms spread. A small cluster spread is correlated with a large number of clusters and vice-versa. Moreover, we observe a typical number of clusters between 5 and 16.

Figures 3g,h show the mean cluster delay and the cluster delay spread, respectively. Note that in our study we are not interested in the absolute delays and thus a constant delay offset due to the measurement equipment was not compensated.

We also compared the scenario at the two frequencies for the OLOS case. Figure 4 shows that the cluster statistics widely match at the two frequencies. This is because of considering only discrete paths. The diffuse components at both frequency bands may be quite different.

VI. CONCLUSIONS

A complete method to parametrise cluster-based geometric stochastic channel models from parametric measurement data is presented. The method uses following steps: (i) identify clusters in measurement data, (ii) identify the optimum number of clusters, (iii) track clusters over consecutive time snapshots, (iv) estimate cluster parameters. For this we introduced a new criterion to find the optimum number of clusters.

Applying this method to indoor measurements, we characterised the cluster parameters by estimated probability density functions of the cluster power, cluster positions (angular and delay), cluster spreads (angular and delay) and the number of paths within a cluster. We divided the measurements in line-of-sight (LOS) and obstructed LOS (OLOS) situations and found significant differences in the parameter statistics. We furthermore show the statistical dependence of selected cluster parameters.

Finally, we compare measurements at centre frequencies of 2.55 GHz and 5.25 GHz and find that the cluster parameters widely match.

To our knowledge, this method is the first one which is able to *automatically* identify, track, and characterise clusters from time-variant measurements.

ACKNOWLEDGEMENTS

We would like to thank Veli-Matti Holappa and Mikko Alatossava for the help with the measurements. This work was conducted within the European Network of Excellence for Wireless Communications (NEWCOM). We thank Elektrobitt Testing Ltd. for generous support.

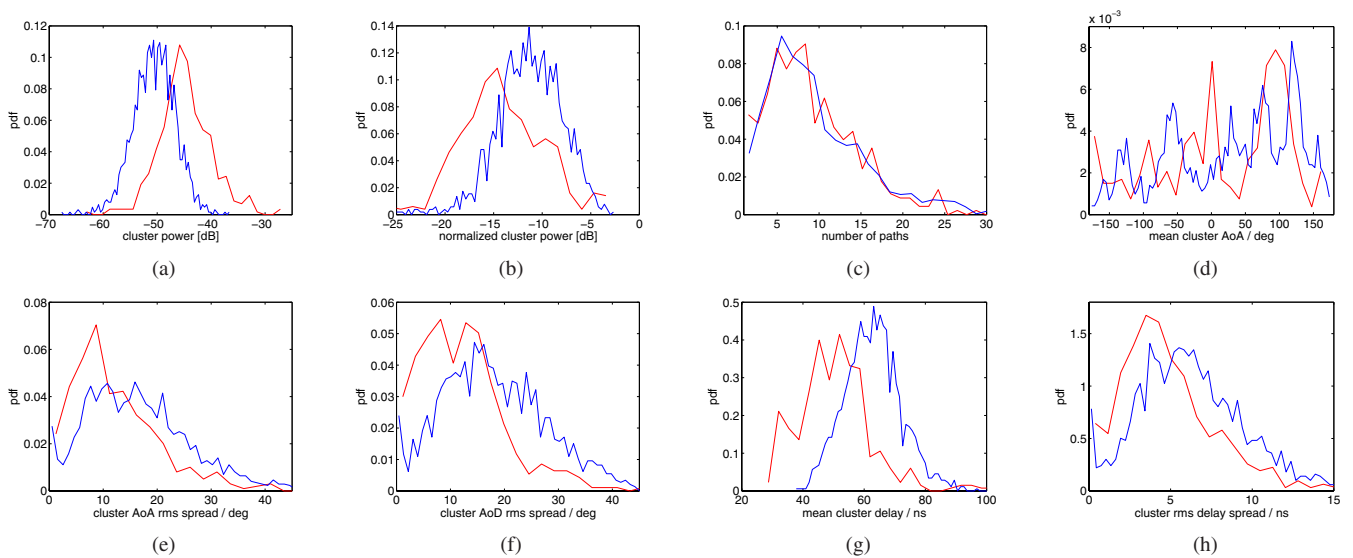


Fig. 3. PDFs of the cluster parameters; red: LOS, blue: OLOS

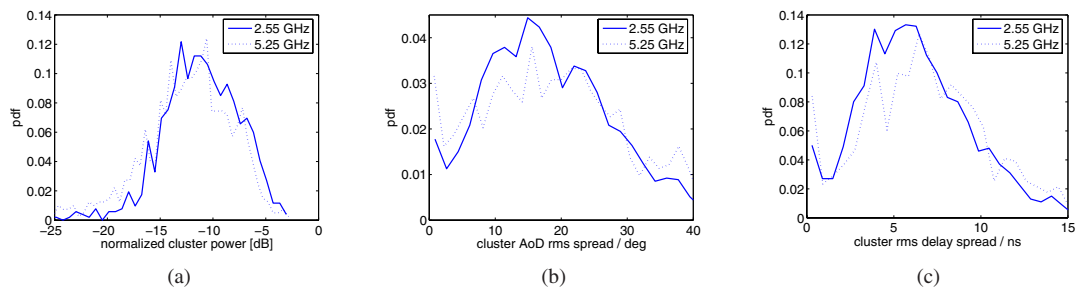


Fig. 4. Comparison of selected cluster parameter statistics for 2.55 GHz (solid lines) and 5.25 GHz (dotted lines).

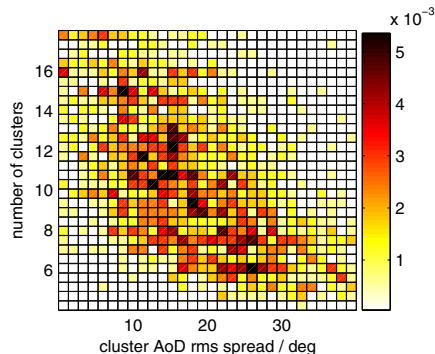


Fig. 5. Joint pdf of the AoD cluster spread and the number of coexistent clusters; hot colours indicate high probability.

REFERENCES

- [1] Q. H. Spencer, B. D. Jeffs, M. A. Jensen, and A. L. Swindlehurst, "Modeling the statistical time and angle of arrival characteristics of an indoor multipath channel," *IEEE Journal on Selected Areas in Communications*, vol. 18, pp. 347 – 359, March 2000.
- [2] C.-C. Chong, C.-M. Tan, D. Laurenson, S. McLaughlin, M. Beach, and A. Nix, "A new statistical wideband spatio-temporal channel model for 5-GHz band WLAN systems," *IEEE Journal on Selected Areas in Communications*, vol. 21, no. 2, pp. 139 – 150, Feb. 2003.
- [3] K. Yu, Q. Li, D. Cheung, and C. Prettie, "On the tap and cluster angular spreads of indoor WLAN channels," in *Proceedings of IEEE Vehicular Technology Conference Spring 2004*, Milano, Italy, May 17–19, 2004.
- [4] K. Li, M. Ingram, and A. Van Nguyen, "Impact of clustering in statistical indoor propagation models on link capacity," *IEEE Transactions on Communications*, vol. 50, no. 4, pp. 521 – 523, April 2002.
- [5] L. Correia, Ed., *Mobile Broadband Multimedia Networks*. Academic Press, 2006.
- [6] J. Salo, J. Salmi, N. Czink, and P. Vainikainen, "Automatic clustering of nonstationary MIMO channel parameter estimates," in *ICT'05*, Cape Town, South Africa, May 2005, Cape Town, South Africa.
- [7] U. Maulik and S. Bandyopadhyay, "Performance evaluation of some clustering algorithms and validity indices," *IEEE Trans. Pattern Analysis and Machine Intelligence*, vol. 24, no. 12, pp. 1650–1654, Dec. 2002.
- [8] N. Czink, P. Cera, J. Salo, E. Bonek, J.-P. Nuutinen, and J. Ylitalo, "Automatic clustering of MIMO channel parameters using the multipath component distance measure," in *WPMC'05*, Aalborg, Denmark, 2005.
- [9] N. Czink and P. Cera, "A novel framework for clustering parametric MIMO channel data including MPC powers," in *COST 273 Post-Project Meeting*, Lisbon, Portugal, Nov. 2005, available at <http://www.nt.tuwien.ac.at/staff/nicolai-czink/>.
- [10] A. Richter, "Estimation of radio channel parameters: Models and algorithms," Ph.D. dissertation, Technische Universität Ilmenau, 2005.
- [11] N. Czink and G. Del Galdo, "Validating a novel automatic cluster tracking algorithm on synthetic IImProp time-variant MIMO channels," in *COST 273 Post-Project Meeting*, Lisbon, Portugal, Nov. 2005, available at <http://www.nt.tuwien.ac.at/staff/nicolai-czink/>.
- [12] L. Hentilä, P. Kyösti, J. Ylitalo, X. Zhao, J. Meinilä, and J.-P. Nuutinen, "Experimental characterization of multi-dimensional parameters at 2.45 and 5.25 GHz indoor channels," in *WPMC2005*, Aalborg, Denmark, September 2005, see also <http://www.propsim.com/>.
- [13] B. Fleury, P. Jourdan, and A. Stucki, "High-resolution channel parameter estimation for MIMO applications using the SAGE algorithm," in *2002 International Zurich Seminar on Broadband Communications*, Zurich, Feb. 2002, pp. 30–1 – 30–9.